

# Isotropic and anisotropic Landau level transitions in epitaxial graphene revealed by infrared optical Hall effect

P. Kühne,\* M. Schubert, and T. Hofmann

*Department of Electrical Engineering and Center for Nanohybrid Functional Materials, University of Nebraska-Lincoln, U.S.A.*

V. Darakchieva and R. Yakimova

*Department of Physics, Chemistry and Biology, IFM, Linköping University, SE-581 83 Linköping, Sweden*

J.D. Tedesco

*ABB, Inc. 171 Industry Drive, P.O. Box 38Bland, VA 24315, U.S.A.*

R.L. Myers-Ward, C.R. Eddy Jr., and D.K. Gaskill

*U.S. Naval Research Laboratory, Washington, DC 20375, U.S.A.*

C.M. Herzinger and J.A. Woollam

*J.A. Woollam Co., Inc., 645 M Street, Suite 102, Lincoln, NE 68508-2243, U.S.A.*

We report on polarization property discrimination of inter Landau level transitions using reflection-type optical Hall effect measurements from 600 to 4000  $\text{cm}^{-1}$  on epitaxial graphene grown by thermal decomposition of silicon carbide. We observe symmetric and anti-symmetric signatures in our data due to unpolarized, i.e., isotropic, and polarized, i.e., anisotropic Landau level transitions, respectively. The isotropic transitions shift with square-root magnetic field dependence typical for stacks of decoupled graphene mono-layers. The anisotropic Landau transitions match those previously observed in Bernal stacked bi-layer graphene, and predicted recently for Bernal stacked tri-layer graphene. The anisotropic signatures can be explained by coupling with free charge carrier magneto-optic plasma oscillations within the transition layer at the substrate graphene interface.

Epitaxial graphene grown by thermal decomposition onto SiC substrates has received tremendous interest due to its unique physical and electronic properties.[1–7] In particular, infrared magneto-optical spectroscopy has been widely applied to probe the electronic states of graphene in the vicinity of the Dirac point, the Fermi velocity and the mobility of free charge carriers which behave as quasi Dirac particles, for instance.[1, 2, 8–10] However, despite these efforts the experimental determination of the complex-valued magneto-optic permittivity tensor  $\epsilon^{\text{MO}}$  in the quantum regime which governs these effects has not been reported so far. The on-diagonal  $\epsilon^{\text{MO}}$  components are conveniently accessible by experiment and have been successfully related to the graphene bandstructure.[11, 12] On the other hand, information on the off-diagonal  $\epsilon^{\text{MO}}$  components is scarce although these elements have been predicted to yield crucial information particularly when probing multilayer graphene.[13] Faraday rotation measurements at infrared wavelengths currently offer the most comprehensive insight, and giant Faraday rotation effects and correlations with the Dirac Landau level structure were reported.[14–16] Faraday experiments provide rotation and intensity, and allow for partial determination of  $\epsilon^{\text{MO}}$  only. For full access to  $\epsilon^{\text{MO}}$ , required to evaluate the polarization properties of Landau transitions in epitaxial graphene, independent information for on- and off-diagonal components of  $\epsilon^{\text{MO}}$  must be obtained from experiment. Sufficient information is provided by optical Hall effect measurements, as discussed in this letter.[17, 18] We report here on our observation of isotropic and anisotropic Landau transitions from optical Hall effect measurements which differ in their magnetic field dependencies, and we discuss possible physical ori-

gins by reconstructing  $\epsilon^{\text{MO}}$  using simple model scenarios.

The optical Hall effect determines changes of optical properties of thin film samples under the influence of external magnetic fields.[18–20] In contrast to Faraday rotation, measurements are conveniently taken in reflection-type arrangement at oblique angle of incidence, thereby discriminating between parallel and perpendicular polarization. Measurements are performed in the Stokes vector approach, and results are reported in the Mueller matrix presentation, which allows immediate differentiation between polarization conserving (isotropic) as well as polarization cross-coupling (anisotropic) sample properties. Subsequent data analysis using model approaches for the dielectric function, or equivalently the optical conductivity, permits quantitative access to physical model parameters. In the Stokes formalism the Mueller matrix  $\mathbf{M}$  connects the Stokes vector of incident and reflected electromagnetic waves  $\mathbf{S}^{\text{in}}$  and  $\mathbf{S}^{\text{out}}$ , respectively, where  $\mathbf{S}^{\text{out}} = \mathbf{M}\mathbf{S}^{\text{in}}$  [21]. The optical Hall effect determines magnetic field-induced differences  $\delta\mathbf{M}$  with respect to  $\mathbf{M}$  at zero field.  $\delta\mathbf{M}$  contains non-zero on-diagonal block elements only ( $\delta M_{11}, \delta M_{12}, \delta M_{21}, \delta M_{22}, \delta M_{33}, \delta M_{34}, \delta M_{43}, \delta M_{44}$ ) when the magnetic field induced sample response is purely isotropic (no cross-polarization), and additional, non-zero off-diagonal block elements ( $\delta M_{13}, \delta M_{31}, \delta M_{14}, \delta M_{41}, \delta M_{23}, \delta M_{32}, \delta M_{24}, \delta M_{42}$ ) when the magnetic field induced sample response is anisotropic, i.e., polarization mode coupling occurs.[21] We note that in our setup elements of both 4<sup>th</sup> row and column are inaccessible, and all remaining elements are normalized by  $M_{11}$  removing light source base line fluctuations, providing 8 independent information.

The epitaxial graphene sample investigated in this let-

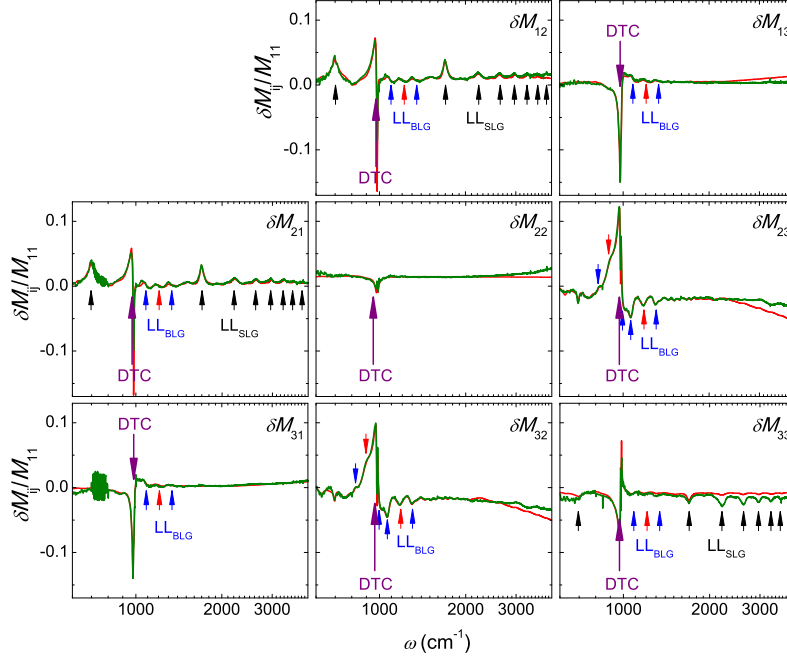


FIG. 1. Optical Hall effect experimental data (green) and best-model fit data (red) for epitaxial graphene at  $B_c = +(5.66 \pm 0.02)$  T and  $T = 1.5$  K. The angle of incidence is  $\Phi_a = 45^\circ$ . DTC, BLG and SLG denote contributions assigned in this letter to Drude-type carriers (DTC), bi-layer graphene LL (BLG) and single-layer graphene LL (SLG), respectively. Signatures indicated by SLG are isotropic and do not occur in off-diagonal-block elements  $\delta M_{32}$ ,  $\delta M_{32}$ ,  $\delta M_{32}$ , and  $\delta M_{32}$ , while features labeled with DTC and BLG are anisotropic and cause cross-polarization.

ter was grown by sublimation on the C-polar (000 $\bar{1}$ ) surface of a semiinsulating 6H-SiC substrate. During the growth, the SiC substrate was heated to 1400  $^\circ$ C in argon atmosphere. Further information on growth conditions can be found in Ref. 22. Optical Hall effect measurements were carried out at  $\Phi_a = 45^\circ$  angle of incidence in the spectral range from 600 to 4000  $\text{cm}^{-1}$  with spectral resolution of 1  $\text{cm}^{-1}$ . [17] The sample was held at temperature  $T = 1.5$  K. The magnetic field was varied from  $B = 0$  T to 8 T in 0.1 T increments while the magnetic field direction was parallel to the reflected beam resulting in a magnetic field  $B_c = B/\sqrt{2}$  parallel to the sample normal. Quantitative optical Hall-effect data analysis requires stratified layer model calculations in which parameterized dielectric functions are used. Least-square principle methods are employed in order to vary model parameters until calculated and experimental ellipsometric data are matched as closely as possible (best-model). [23] The dielectric functions for silicon carbide are composed of Lorentzian-broadened oscillators described by the respective longitudinal-optical (LO) and transverse-optical (TO) phonon frequencies. [24]

Figure 1 depicts results of optical Hall effect measurements at  $B_c = +(5.66 \pm 0.02)$  T. Graphs are arranged according to their appearance in the Mueller matrix, with the top left corner ( $\delta M_{11}$ ) omitted. The spectral response observed in the on-diagonal block elements is distinctly different from the off-diagonal block response. Comparing representative elements, e.g.,  $\delta M_{33}$  and  $\delta M_{32}$ , two sets of pronounced resonances which we attribute below to Landau level transitions, can be identified. The first set of transitions, indicated with vertical arrows labeled  $\text{LL}_{\text{SLG}}$ , is isotropic, i.e., not associated with cross-polarization, and spread out over the entire measured spectral range. These transitions do not occur in off-diagonal block elements. The term “SLG” stands for single-layer graphene. The second set of resonances, indicated with vertical arrows labeled  $\text{LL}_{\text{BLG}}$ , is anisotropic, i.e., associated with cross-polarization, and occurs in a

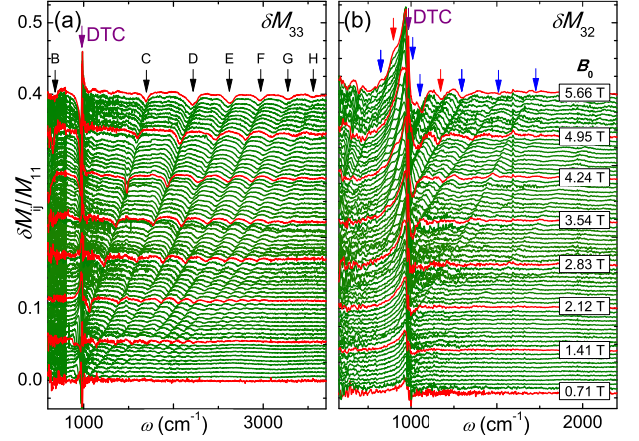


FIG. 2. Selected on- and off-diagonal-block optical Hall-effect spectra ( $T = 1.5$  K,  $\Phi_a = 45^\circ$ ) for  $B_c = +(0.707 \pm 0.002)$  T to  $B_c = +(5.66 \pm 0.02)$  T in 0.07 T increments. The graphs are stacked by 0.006. (a)  $\delta M_{33}$ ; Isotropic Landau level transitions, indicated by letters according to Sadowski *et al.* (b)  $\delta M_{32}$ ; Anisotropic Landau transitions, indicated by blue and red arrows.

narrower range from 600 to 1500  $\text{cm}^{-1}$ . The term “BLG” indicates bilayer-layer graphene, however, as will be discussed below, a subset of these transitions will be assigned to tri-layer graphene. In addition, a pronounced feature observed at 970  $\text{cm}^{-1}$ , indicated with vertical arrows and labeled by DTC, is common to all graphs in Fig. 1 and hence anisotropic. The term “DTC” stands for Drude-type carriers.

Non-zero off-diagonal block Mueller matrix elements are inherently tied to the existence of off-diagonal components in  $\epsilon^{\text{MO}}$ . Thus, a priori, one must conclude that transitions  $\text{LL}_{\text{SLG}}$  originate from processes in sample regions with polarizability contributions to  $\epsilon^{\text{MO}}$  that are diagonal and hence isotropic. Likewise, transitions  $\text{LL}_{\text{BLG}}$  are to be described by contributions with non-diagonal components in  $\epsilon^{\text{MO}}$ . Without loss of generality, the optical response of electronic systems with bound and unbound excitations subjected to external magnetic fields

can be constructed by using magneto-optic polarizability functions  $\chi_+$  and  $\chi_-$  for right- and left-handed circularly polarized light, respectively.[19] In Cartesian coordinates  $\epsilon^{\text{MO}}$  is then anti-symmetric:

$$\epsilon^{\text{MO}} = \mathbf{I} + \frac{1}{2} \begin{pmatrix} (\chi_+ + \chi_-) & i(\chi_+ - \chi_-) & 0 \\ -i(\chi_+ - \chi_-) & (\chi_+ + \chi_-) & 0 \\ 0 & 0 & 0 \end{pmatrix}, \quad (1)$$

where  $\mathbf{I}$  indicates the unit matrix and the magnetic field is taken along the z-direction. All other dielectric contributions are omitted. For  $\chi_+ \neq \chi_-$ ,  $\epsilon^{\text{MO}}$  describes a medium with anisotropic magneto-optical properties which produce non-vanishing off-diagonal block elements in the optical Hall effect, whereas for  $\chi_+ = \chi_-$ ,  $\epsilon^{\text{MO}}$  describes a medium with isotropic magneto-optical properties, and off-diagonal block elements in the optical Hall effect do not occur. Hence, for transitions  $\text{LL}_{\text{SLG}}$   $\chi_+ = \chi_-$ , while for  $\text{LL}_{\text{BLG}}$   $\chi_+ \neq \chi_-$ . A semi-classical description for  $\chi_{\pm}$  can be obtained using  $n$  series of Lorentzian-broadened Green functions at energies  $\hbar\omega_{0,n}$  with spectral weight  $\omega_{p,n}^2$ , scattering life time  $1/\gamma_n$  and including coupling to a magneto-optic plasma mode  $\omega_c$

$$\chi_{\pm} = \sum_n \omega_{p,n}^2 (\omega_{0,n}^2 - \omega^2 - i\omega\gamma_{p,n} \pm i\omega\omega_c)^{-1}. \quad (2)$$

When the plasma coupling is turned off, i.e.,  $\omega_c \rightarrow 0$ ,  $\epsilon^{\text{MO}}$  becomes symmetric. Standard layer model calculations to determine the Mueller matrix elements of epitaxial graphene on silicon carbide using Eqs. (1) and (2) reproduce lineshape and isotropy of all features labeled  $\text{LL}_{\text{SLG}}$  in Fig. 1. When coupling with plasma modes is considered, i.e.,  $\omega_c > 0$ , features are mapped out onto the off-diagonal-block elements, and lineshapes match excellently with the experimental data for transitions labeled by  $\text{LL}_{\text{BLG}}$ .

Figure 2 summarizes on-diagonal and off-diagonal-block Mueller matrix difference spectra as a function of the magnetic field. The anisotropic resonance at  $970 \text{ cm}^{-1}$ , labeled with DTC, increases in amplitude with increasing magnetic field strength. The wavenumber at which this resonance occurs does not vary with the external magnetic field strength. The physical origin of this resonance is the coupled motion of bound charge displacement near the longitudinal optical phonon mode of the silicon carbide substrate with a free charge carrier plasma at the sample surface producing resonant magneto-optic birefringence.[19, 23, 25] Eqs. 1 and 2 can be used to render this phenomenon when  $\hbar\omega_0$  is the (bound) phonon mode energy. The resulting polarization contribution is anisotropic and occurs in all Mueller matrix elements. We attribute this mode to highly doped graphene layers in close vicinity of the interface between the substrate and the epitaxial graphene, originating from SiC charge transfer. [26]

The magnetic field-dependent measurements reveal that energy spacings of transitions  $\text{LL}_{\text{SLG}}$  scale with the square root of transition index  $n$  and magnetic field  $B$ , indicative for the Dirac-type bandstructure with Fermi level close to the charge neutrality point.[8] Data in Fig. 3 (a) are parameters  $\omega_{0,n}$  obtained from best-match

model analysis of the optical Hall effect spectra as a function of  $B_c$ . We attribute these transition to originate within regions of the epitaxial graphene that are composed of decoupled, quasi neutral graphene sheets.[9] Energies in Fig. 3 (a) follow  $E_{\text{SLG}}^{\text{LL}}(n) = \text{sign}(n)E_0\sqrt{|n|}$  with  $E_0 = \tilde{c}\sqrt{2\hbar e\mu_0|B_c|}$  and average velocity of Dirac fermions  $\tilde{c}$ . The naming convention used to indicate transitions in Fig. 3(a) is adapted from Sadowski *et al.*[27] Optical selection rules for transitions between levels  $n'$  and  $n$  require  $|n'| = |n| \pm 1$ . The best-match model velocity obtained from matching all data in Fig. 3 (a) is  $\tilde{c} = (1.01 \pm 0.01) \times 10^6 \text{ m/s}$ , in very good agreement with Refs. 8–10, 14, 28, and 29. The corresponding best-match functions  $E_{\text{SLG}}^{\text{LL}}$  versus  $B_c$  are plotted as solid lines in Fig. 3 (a).

Transition energy parameters obtained from best-match model analysis of the off-diagonal-block optical Hall effect data are plotted in Fig. 3 (b) and exhibit sub-linear behavior. The magnetic field scaling of the energy spacings for the anisotropic transitions suggests bi- and tri-layer graphene as their physical origin. The transition energies of N-layer graphene have been described as [10, 30, 31]

$$E_{\text{N-BLG}}^{\text{LL}}(n, \mu) = \text{sign}(n) \frac{1}{\sqrt{2}} \left[ (\lambda_N \gamma)^2 + (2|n| + 1) E_0^2 + \mu \sqrt{(\lambda_N \gamma)^4 + 2(2|n| + 1) E_0^2 (\lambda_N \gamma)^2 + E_0^4} \right]^{1/2}, \quad (3)$$

with coupling constant  $\gamma$ , layer parameter  $\lambda_N$  [31] and where  $\mu = -1, +1$  corresponds to the higher and lower subbands in the limit of zero magnetic field, respectively.[31] Optical selection rules are the same as for  $E_{\text{SLG}}^{\text{LL}}(n)$ . Using  $\tilde{c} = (1.01 \pm 0.01) \times 10^6 \text{ m/s}$ , best-match model functions are plotted in Fig. 3(b) for  $N = 2$  and  $N = 3$  as blue solid and red dashed lines, respectively. No transition was observed that would correspond to  $N > 3$ . These transitions can be assigned to Bernal stacked bi-layer graphene ( $N = 2$ ) and tri-layer graphene ( $N = 3$ ). The best-match model parameters obtained here are  $\gamma = (3120 \pm 175) \text{ cm}^{-1}$  for  $N = 2$ , corroborating the result obtained by Orlita *et al.* from FTIR transmission experiments.[10] For  $N = 3$ , we observe  $\gamma = (3150 \pm 20) \text{ cm}^{-1}$ , which render the first experimental confirmation of the theoretical predictions by Koshino and Ando for tri-layer graphene. [31] We note that these anisotropic Landau transitions are only observed and resolved for  $n = 2 \dots 6$  for bi-layer graphene, and for  $n = 4$  and  $n = 5$  for tri-layer graphene. At this point, we do not know why transitions with  $n > 6$  for  $N = 2$  and  $n \neq 4, n \neq 5$  for  $N = 3$  cannot be observed. However, the fact that these transitions appear with anisotropic optical Hall effect signatures suggests their coupling with free charge carriers within the sample. We propose that stacking order defects within the bi-layer and tri-layer graphene allow for coupling of Dirac particles within their Landau levels with the cyclotron resonance [15] of the free carrier plasma resulting in anisotropic Landau transition signatures.

In conclusion, we determine for the first time the full polarization properties of Landau transitions in epitax-



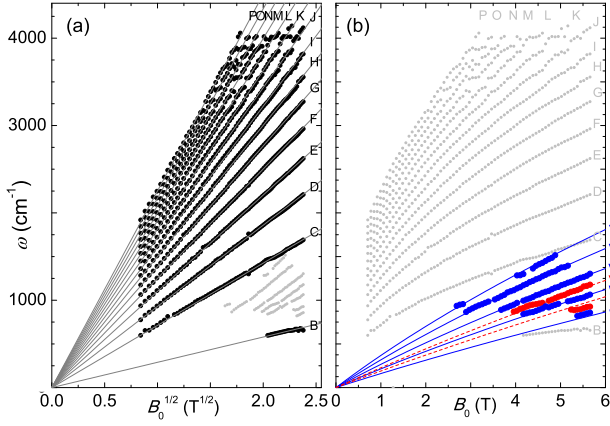


FIG. 3. Symmetric (a; isotropic) and anti-symmetric (b; anisotropic) Landau transition energies in epitaxial graphene determined from optical Hall effect measurements at 1.5 K. Solid lines denote single-layer graphene (a; black), bi-layer (b; blue) and tri-layer graphene (b; red) dependencies on the magnetic field.

ial graphene using the optical Hall effect. Magnetic-field dependent measurements revealed that isotropic transitions originate from decoupled graphene mono-layers, while anisotropic transitions reflect dependencies previously recorded for bi-layer graphene. Furthermore, we observe anisotropic transitions previously predicted for tri-layer graphene. The anisotropic transitions correspond to optical conductivity contributions with non-vanishing off-diagonal tensor components. We suggest that Landau transitions, while intrinsically isotropic, produce anisotropic conductivity contributions when coupling occurs between Landau levels and free charge carrier modes. We suggest that such coupling may be promoted via stacking defects in bi-layer and tri-layer graphene. The knowledge of the polarization dependent optical response of Landau-level transitions is found invaluable for accurate assignment of the origin of the Landau transitions occurring in epitaxial graphene.

The authors would like to acknowledge financial support from the Army Research Office (D. Woollard, Contract No. W911NF-09-C-0097), the National Science Foundation (Grant Nos. MRSEC DMR-0820521, MRI DMR-0922937, DMR-0907475), the University of Nebraska-Lincoln, the J.A. Woollam Foundation, the Office of Naval Research, the Swedish Research Council (VR) under grant No.2010-3848 and, the Swedish Governmental Agency for Innovation Systems (VINNOVA) under the VINNMER international qualification program, grant No.2011-03486.

\* kuehne@huskers.unl.edu; <http://ellipsometry.unl.edu>

- [1] C. Berger, Z. Song, T. Li, X. Li, A. Y. Ogbazghi, R. Feng, Z. Dai, A. N. Marchenkov, E. H. Conrad, P. N. First, and W. A. de Heer, *J. Phys. Chem. B* **108**, 19912 (2004).
- [2] C. Berger, Z. Song, X. Li, X. Wu, N. Brown, C. Naud, D. Mayou, T. Li, J. Hass, A. N. Marchenkov, E. H. Conrad, P. N. First, *et al.*, *Science* **312**, 1191 (2006).
- [3] C. Virojanadara, M. Syvaearja, R. Yakimova, L. I. Johansson, A. A. Zakharov, and T. Balasubramanian, *Phys. Rev. B* **78**, 245403 (2008).
- [4] Y.-M. Lin, H.-Y. Chiu, K. A. Jenkins, D. B. Farmer, P. Avouris, and A. Valdes-Garcia, *IEEE Electron. Device Letters* **31**, 68 (2010).
- [5] W. de Heer, C. Berger, M. Ruan, M. Sprinkle, X. Li, Y. Hu, B. Zhang, J. Hankinson, and E. Conrad, *PNAS* **108**, 16900 (2011).
- [6] Y. M. Lin, A. Valdes-Garcia, S. J. Han, D. B. Farmer, I. Meric, C. Dimitrakopoulos, A. Grill, P. A. K. A. Jenkins, *et al.*, *Science* **332**, 6035 (2011).
- [7] Y. Q. Wu, K. A. Jenkins, A. Valdes-Garcia, D. B. Farmer, Y. Zhu, F. M. Xia, P. Avouris, Y. M. Lin, *et al.*, *Nano Lett.* **12**, 3062 (2012).
- [8] M. L. Sadowski, G. Martinez, M. Potemski, C. Berger, and W. A. de Heer, *Phys. Rev. Lett.* **97**, 266405 (2006).
- [9] M. Orlita, C. Faugeras, P. Plochocka, P. Neugebauer, G. Martinez, C. Berger, W. A. de Heer, M. Potemski, *et al.*, *Phys. Rev. Lett.* **101**, 267601 (2008).
- [10] M. Orlita, C. Faugeras, R. Grill, A. Wyszomolek, W. Strupinski, C. Berger, W. A. de Heer, *et al.*, *Phys. Rev. Lett.* **107**, 216603 (2011).
- [11] L. M. Zhang, Z. Q. Li, D. N. Basov, M. M. Fogler, Z. Hao, and M. C. Martin, *Phys. Rev. B* **78**, 235408 (2008).
- [12] Z. Q. Li, E. A. Henriksen, Z. Jiang, Z. Hao, M. C. Martin, P. Kim, H. L. Stormer, and D. N. Basov, *Phys. Rev. Lett.* **102**, 037403 (2009).
- [13] T. Morimoto, M. Koshino, and H. Aoki, *Phys. Rev. B* **86**, 155426 (2012).
- [14] E. A. Henriksen, Z. Jiang, L.-C. Tung, M. E. Schwartz, M. Takita, Y.-J. Wang, P. Kim, and H. L. Stormer, *Phys. Rev. Lett.* **100**, 087403 (2008).
- [15] I. Crassee, J. Levallois, A. L. Walter, M. Ostler, A. Bostwick, E. Rotenberg, T. Seyller, D. van der Marel, and A. B. Kuzmenko, *Nat Phys* **7**, 48 (2011).
- [16] I. Crassee, J. Levallois, D. van der Marel, A. L. Walter, T. Seyller, and A. B. Kuzmenko, *Phys. Rev. B* **84**, 035103 (2011).
- [17] T. Hofmann, U. Schade, W. Eberhardt, C. M. Herzinger, P. Esquinazi, and M. Schubert, *Rev. Sci. Instrum.* **77**, 63902 (2006).
- [18] T. Hofmann, C. M. Herzinger, J. L. Tedesco, D. K. Gaskill, J. A. Woollam, and M. Schubert, *Thin Solid Films* **519**, 2593 (2011).
- [19] M. Schubert, T. Hofmann, and C. M. Herzinger, *J. Opt. Soc. Am. A* **20**, 347 (2003).
- [20] T. Hofmann, C. Herzinger, and M. Schubert, *phys. stat. sol. (a)* **205**, 779 (2008).
- [21] H. Fujiwara, *Spectroscopic Ellipsometry* (John Wiley & Sons, New York, 2007).
- [22] J. L. Tedesco, G. G. Jernigan, J. C. Culbertson, J. K. Hite, Y. Yang, K. M. Daniels, R. L. Myers-Ward, C. R. Eddy, *et al.*, *Appl. Phys. Lett.* **96**, 222103 (2010).
- [23] M. Schubert, *Infrared Ellipsometry on semiconductor layer structures: Phonons, plasmons and polaritons*, vol. 209 of *Springer Tracts in Modern Physics* (Springer, Berlin, 2004).
- [24] T. E. Tiwald, J. A. Woollam, S. Zollner, J. Christiansen, R. B. Gregory, T. Wetteroth, S. R. Wilson, and A. R. Powell, *Phys. Rev. B* **60**, 11464 (1999).
- [25] M. Schubert, T. Hofmann, and J. Šik, *Phys. Rev. B* **71**, 35324 (2005).
- [26] Y.-M. Lin, C. Dimitrakopoulos, D. B. Farmer, S.-J. Han, Y. Wu, W. Zhu, D. K. Gaskill, J. L. Tedesco, R. L. Myers-Ward, J. Charles R. Eddy, A. Grill, and P. Avouris, *Appl. Phys. Lett.* **97**, 112107 (2010).
- [27] M. Sadowski, G. Martinez, M. Potemski, C. Berger, and W. de Heer, *Solid State Commun.* **143**, 123 (2007).
- [28] M. Orlita, C. Faugeras, J. Borysiuk, J. M. Baranowski, W. Strupinski, M. Sprinkle, C. Berger, W. A. de Heer, D. M. Basko, G. Martinez, and M. Potemski, *Phys. Rev. B* **83**, 125302 (2011).

- [29] M. Orlita, C. Faugeras, J. M. Schneider, G. Martinez, D. K. Maude, and M. Potemski, Phys. Rev. Lett. **102**, 166401 (2009).
- [30] D. S. L. Abergel and V. I. Fal'ko, Phys. Rev. B **75**, 155430 (2007).
- [31] M. Koshino and T. Ando, Phys. Rev. B **77**, 115313 (2008).